Parametric Response Mapping Adds Value to Current Computed Tomography Biomarkers in Diagnosing Chronic Obstructive Pulmonary Disease

To the Editor:

Lung function testing is the gold standard for diagnosing and classifying chronic obstructive pulmonary disease (COPD), although it may not capture the heterogeneity of the disease completely (1). Different quantitative methods based on computed tomography (CT) of the lungs have been proposed to untangle the different pathological mechanisms involved (2).

Recently, a new CT-based biomarker was reported that provides visualization and quantification of COPD phenotypes in patients with COPD (3). This so-called parametric response mapping (PRM) is a voxel-based image-analysis technique for evaluating both inspiratory and expiratory CT scans. It provides a color map, which represents normal lung tissue, small airway disease, or emphysema, and gives insight into the extent and localization of disease.

Thus far, only one study has described the association of PRM with lung function, showing moderate to good correlations (3). However, whether PRM adds additional value to current CT-based biomarkers in diagnosing COPD is unknown. We hypothesized that PRM could have added value because of its ability to distinguish between air trapping related to emphysema and air trapping related to small airway disease. The aim of this study was to evaluate the added diagnostic value of PRM in evaluating COPD based on CT.

We analyzed participants taking part in the Dutch and Belgian Lung Cancer Screening Trial (NELSON). Only participants from the University Medical Center Utrecht were included because they underwent both inspiratory and expiratory CT. Inclusion and exclusion criteria have been reported before (4). In short, all participants were current or former smokers with a smoking history of at least 16.5 pack-years and age between 50 and 75 years.

All participants underwent prebronchodilator pulmonary function tests according to the European Respiratory Society/American Thoracic Society guidelines (5). FEV_1 and FVC were recorded. COPD was defined according to the Global Initiative for Chronic Obstructive Lung Disease (GOLD) criteria (6).

Low-dose volumetric CT scans were made with 16×0.75 mm collimation (Brilliance 16P; Philips Medical Systems, Cleveland, OH). Emphysema was assessed by the 15th percentile (Perc15) technique (7). Perc15 represents the Hounsfield unit (HU) point below which 15% of the voxels are distributed. The closer Perc15 is to −1,000, the more emphysema is present. Airway wall thickness was calculated by the square root of wall area for a theoretical airway with an internal perimeter of 10 mm (Pi10) (8–10). Air trapping was assessed using the mean expiratory to inspiratory ratio of the mean lung density ($E/I\text{-ratio}_{MLD}$) (11). PRM measurements were implemented as a joint histogram analysis between inspiratory and expiratory scans after image registration (12, 13). Lung segmentation was visually checked. Applying the standard thresholds of −950 HU for emphysema in the inspiratory acquisition and −856 HU in the expiratory acquisition to define air trapping, PRM is summarized in three quantities: all voxels with HU below −950 in the inspiratory CT and below −856 in the expiratory CT represent emphysema (PRM^{Emph}), all voxels above −950 in the inspiratory CT and below −856 in the expiratory CT represent air trapping (PRM^{fSAD}), and all voxels above both thresholds in both scans represent normal lung (PRM^{Norm}) (see Figure 1). Measurements were corrected for lung volume.

A multivariate logistic regression model was developed with COPD status (absent or present) as outcome. Prior to this analysis, PRM measurements were log transformed to obtain normally distributed data. The baseline model included age, body mass index, smoking status, and pack-years. In subsequent models, Pi10, Perc15, $E/I\text{-ratio}_{MLD}$, and PRM measurements were added one at a time. Models were compared by the log-likelihood ratios test. The ability to discriminate between participants with and without COPD was assessed by calculating the area under the receiver operating characteristic curve (i.e., C-statistic). Reclassification of participants' COPD status was calculated. Additional gas transfer analyses were performed by using diffusing capacity of the lung for carbon monoxide and K_{CO} values in a subgroup of our cohort to gain insight into the possible clinical relevance of PRM.

A total of 1,140 male participants were included; 87 participants were excluded because of lung segmentation errors, and 6 participants were excluded because of negative inspiratory–expiratory differences, resulting in 1,047 eligible participants for analysis. Excluded participants (n = 93) had a mean (SD) age of 64.7 (6.3) years, and included participants (n = 1,047) had a mean (SD) age of 62.4 (5.1) years ($P < 0.001$). Median (25–75th percentile) pack-years of excluded participants were 46.4 (32.2–54.2), and median (25–75th percentile) pack-years of included participants were 40.5 (28.0–49.5; $P = 0.01$). There were no significant differences in body mass index, smoking status, FEV_1, and COPD status ($P = 0.47$, $P = 0.43$, $P = 0.81$, and $P = 0.10$, respectively). Three hundred ninety-four (37.6%) participants were classified as having COPD, of whom 251 (23.9%) were classified as GOLD 1, 121 (11.6%) as GOLD 2, and 22 (2.1%) as GOLD 3.

Compared with the baseline model, the model improved significantly when CT-derived biomarkers (Pi10, Perc15, $E/I\text{-ratio}_{MLD}$, and PRM) were added one by one (Table 1). The baseline model with PRM had the highest diagnostic value (C-statistic of 0.827). When adding all three current CT-derived biomarkers (Pi10, Perc15, and $E/I\text{-ratio}_{MLD}$), the resulting C-statistic was 0.877. The addition of PRM to the latter model led to a further significant increase in the ability to discriminate between participants with and without COPD (C-statistic: 0.883, $P < 0.001$). Reclassification analyses showed that this model had the least falsely reclassified participants of all models (193; 18,4%). Reclassification results are shown in Table 1.

Of 1,047 participants, 493 underwent gas transfer measurements. When selecting the upper quintile of PRM^{Emph} (n = 99), 27 (27.3%) participants of this subgroup had normal gas transfer. This could mean that a substantial group of participants with normal gas transfer could already have signs of smoking-related changes on CT measured with PRM. In Table E1 in the

Author Contributions: Conception and design: E.P., E.M.v.R., M.S., J.R., L.G.E., R.V., M.O., H.J.d.K., B.v.G., P.A.d.J., J.-W.J.L., and F.A.A.M.H.; analysis and interpretation: E.P., E.M.v.R, P.A.d.J., and F.A.A.M.H; drafting the manuscript for important intellectual content: E.P., E.M.v.R., M.S., J.R., L.G.E., R.V., M.O., H.J.d.K., B.v.G., P.A.d.J., J.-W.J.L., and F.A.A.M.H.

This letter has an online supplement, which is accessible from this issue's table of contents at www.atsjournals.org

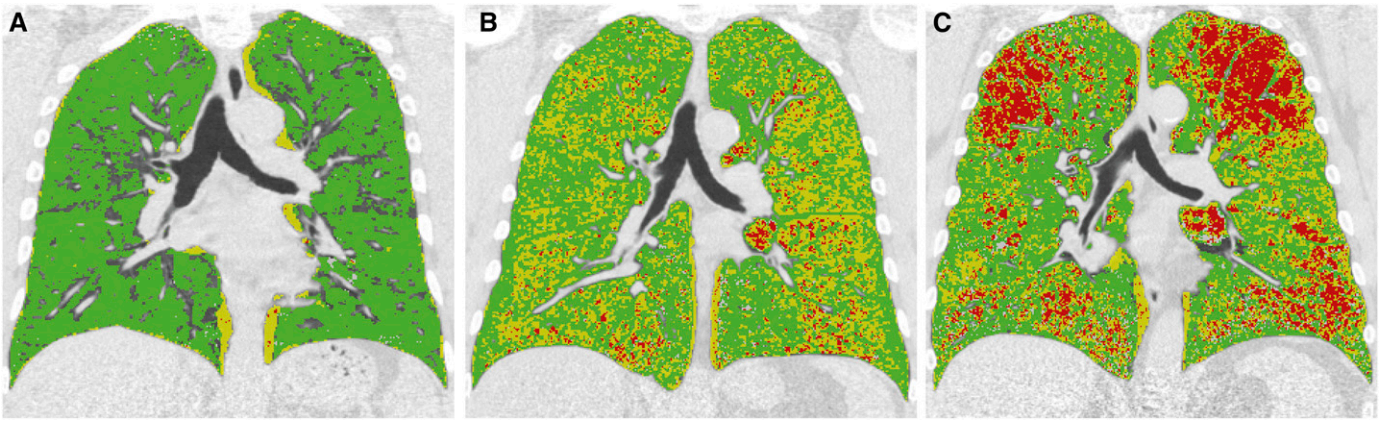

Figure 1. Parametric response mapping (PRM) color map. Inspiratory computed tomography scans with PRM color maps from three different participants, representing normal lung tissue (*green*), small airway disease (*yellow*), and emphysema (*red*). (*A*) Fifty-eight-year-old man without chronic obstructive pulmonary disease (COPD). PRM values were 0.02% PRM^{Emph} and 4.02% PRM^{fSAD}. (*B*) Fifty-nine-year-old man with COPD, Global Initiative for Chronic Obstructive Lung Disease (GOLD) stage 3. The color map shows that airway obstruction is mainly a result of small airway disease, with PRM values of 4.2% PRM^{Emph} and 37.3% PRM^{fSAD}. (*C*) Sixty-one-year-old man with COPD GOLD stage 3. As this PRM map shows, his airway obstruction is the result of both emphysema and small airway disease. PRM measures were 19.4% PRM^{Emph} and 29.4% PRM^{fSAD}. All voxels with Hounsfield units below −950 in the inspiratory CT and below −856 in the expiratory CT represent emphysema (PRM^{Emph}), all voxels above −950 in the inspiratory CT and below −856 in the expiratory CT represent air trapping (PRM^{fSAD}), and all voxels above both thresholds in both scans represent normal lung (PRM^{Norm}).

online supplement, all CT-derived measurements of participants with normal gas transfer are shown as a reference.

Our results show that in this cohort, PRM exceeded other measures in diagnostic value when added as single biomarkers. When adding PRM to all currently available CT-derived biomarkers, this resulted in a significant increase in C-statistic.

Galbán and colleagues (3) is the only group that has studied the use of PRM in quantifying COPD on CT. They found that with decreasing FEV_1, levels of PRM measurements increased. Next to information about the correlation with FEV_1, it is important to evaluate whether PRM assessment contributes to the current CT assessment of COPD. We evaluated this in a large cohort with generally healthy smokers. With the extensive characterization of a high-risk cohort, this study provided valuable information regarding the role of PRM in the assessment of smoking-related changes underlying COPD. We showed that an expiratory scan could provide information about small and large airways in participants with emphysema.

Although the added value of PRM to currently used CT measurements of COPD is important in evaluating PRM as a diagnostic tool, it should be recognized that the clinical relevance of this measurement is still unknown and that it is not yet confirmed by histology. In addition, PRM should be analyzed in a healthy cohort with nonsmoking subjects to provide a normal range of this measurement. With a normal reference standard, the influence of inspiratory–expiratory volume differences could be evaluated and PRM measurements could be compared with both spirometry and gas transfer to assess its clinical relevance.

Table 1. Discrimination of the Various Multivariate Models in the Identification of Chronic Obstructive Pulmonary Disease

	Model	C-Statistic (95% CI)	FP [*n* (%)]	FN [*n* (%)]
1	Baseline*	0.659 (0.625–0.693)	74 (7.1%)	291 (27.8%)
2	+ Pi10	0.763 (0.733–0.793)	97 (9.3%)	189 (18.1%)
3	+ Perc15	0.761 (0.731–0.791)	98 (9.4%)	201 (19.2%)
4	+ $E/I\text{-ratio}_{MLD}$	0.783 (0.755–0.810)	112 (10.7%)	186 (17.8%)
5	+ Pi10 + Perc15	0.864 (0.841–0.887)	72 (6.9%)	128 (12.2%)
6	+ Pi10 + $E/I\text{-ratio}_{MLD}$	0.810 (0.784–0.837)	92 (8.8%)	167 (16.0%)
7	+ Perc15 + $E/I\text{-ratio}_{MLD}$	0.827 (0.802–0.853)	96 (9.2%)	154 (14.7%)
8	+ Pi10 + Perc15 + $E/I\text{-ratio}_{MLD}$	0.877 (0.856–0.899)	75 (7.2%)	127 (12.1%)
9	+ PRM	0.827 (0.802–0.853)	54 (2.2%)	191 (18.2%)
10	+ Pi10 + PRM	0.863 (0.840–0.886)	61 (5.8%)	150 (14.3%)
11	+ Perc15 + PRM	0.826 (0.800–0.852)	63 (6.0%)	183 (17.5%)
12	+ $E/I\text{-ratio}_{MLD}$ + PRM	0.833 (0.808–0.857)	69 (6.6%)	181 (17.3%)
13	+ Pi10 + $E/I\text{-ratio}_{MLD}$ + PRM	0.881 (0.859–0.903)	69 (6.6%)	109 (10.4%)
14	+ Pi10 + Perc15 + $E/I\text{-ratio}_{MLD}$ + PRM	0.883 (0.862–0.904)	69 (6.6%)	124 (11.8%)

Definition of abbreviations: 95% CI = 95th percentile confidence interval; FP = false positives; FN = false negatives; Pi10 = airway wall thickness at an internal perimeter of 10 mm; Perc15 = emphysema score as 15th percentile of attenuation distribution curve on inspiratory scan; $E/I\text{-ratio}_{MLD}$ = expiration-to-inspiration ratio of mean lung density; PRM = parametric response mapping.
*Baseline model consisted of age, body mass index, smoking status, and pack-years.

In conclusion, PRM adds significantly to the diagnostic value of current CT quantification methods in assessing the presence of COPD. It could be helpful in identifying smoking-related changes and might contribute to the effect of lung cancer screening. Therefore, this novel quantification technique deserves further investigation. ■

Author disclosures are available with the text of this letter at www.atsjournals.org.

Esther Pompe, M.D.
University Medical Center Utrecht
Utrecht, the Netherlands

Eva M. van Rikxoort, M.Sc., Ph.D.
Radboud University Medical Center
Nijmegen, the Netherlands

Michael Schmidt
Radboud University Medical Center
Nijmegen, the Netherlands
and
Fraunhofer MEVIS
Bremen, Germany

Jan Rühaak
Fraunhofer MEVIS
Bremen, Germany

Leticia Gallardo Estrella, M.Sc.
Radboud University Medical Center
Nijmegen, the Netherlands

Rozemarijn Vliegenthart, M.D., Ph.D.
Matthijs Oudkerk, M.D., Ph.D.
University of Groningen
Groningen, the Netherlands

Harry J. de Koning, M.D., Ph.D.
Erasmus MC
Rotterdam, the Netherlands

Bram van Ginneken, M.Sc., Ph.D.
Radboud University Medical Center
Nijmegen, the Netherlands

Pim A. de Jong, M.D., Ph.D.
Jan-Willem J. Lammers, M.D., Ph.D.
Firdaus A. A. Mohamed Hoesein, M.D., Ph.D.
University Medical Center Utrecht
Utrecht, the Netherlands

References

1. Agustí A, Vestbo J. Current controversies and future perspectives in chronic obstructive pulmonary disease. *Am J Respir Crit Care Med* 2011;184:507–513.
2. Lynch DA, Newell JD. Quantitative imaging of COPD. *J Thorac Imaging* 2009;24:189–194.
3. Galbán CJ, Han MK, Boes JL, Chughtai KA, Meyer CR, Johnson TD, Galbán S, Rehemtulla A, Kazerooni EA, Martinez FJ, *et al*. Computed tomography-based biomarker provides unique signature for diagnosis of COPD phenotypes and disease progression. *Nat Med* 2012;18: 1711–1715.
4. van Iersel CA, de Koning HJ, Draisma G, Mali WPTM, Scholten ET, Nackaerts K, Prokop M, Habbema JDF, Oudkerk M, van Klaveren RJ. Risk-based selection from the general population in a screening trial: selection criteria, recruitment and power for the Dutch-Belgian randomised lung cancer multi-slice CT screening trial (NELSON). *Int J Cancer* 2007;120:868–874.
5. Miller MR, Crapo R, Hankinson J, Brusasco V, Burgos F, Casaburi R, Coates A, Enright P, van der Grinten CPM, Gustafsson P, *et al*.; ATS/ERS Task Force. General considerations for lung function testing. *Eur Respir J* 2005;26:153–161.
6. Global Initiative for Chronic Obstructive Lung Disease. Global Strategy for Diagnosis, Management, and Prevention of COPD [accessed 2015 Jan 21]. Available from: http://www.goldcopd.org/guidelines-global-strategy-for-diagnosis-management.html
7. Parr DG, Stoel BC, Stolk J, Stockley RA. Validation of computed tomographic lung densitometry for monitoring emphysema in alpha1-antitrypsin deficiency. *Thorax* 2006;61:485–490.
8. Van Rikxoort EM, Baggerman W, van Ginneken B. Automatic segmentation of the airway tree from thoracic CT scans using a multi-threshold approach. *Proc Second Int Workshop Pulmonary Image Anal* 2009:341–349.
9. Mets OM, de Jong PA, van Ginneken B, Gietema HA, Lammers JWJ. Quantitative computed tomography in COPD: possibilities and limitations. *Lung* 2012;190:133–145.
10. van Ginneken B, Baggerman W, Van Rikxoort EM. Robust segmentation and anatomical labeling of the airway tree from thoracic CT scans. *Proc Second Int Workshop Pulmonary Image Anal* 2008;219–226.
11. Mets OM, Zanen P, Lammers JWJ, Isgum I, Gietema HA, van Ginneken B, Prokop M, de Jong PA. Early identification of small airways disease on lung cancer screening CT: comparison of current air trapping measures. *Lung* 2012;190:629–633.
12. Rühaak J, Heldmann S, Kipshagen T, Fischer B. Highly accurate fast lung CT registration. *Proc SPIE Med Imaging* 2013;86690Y:1–9.
13. van Rikxoort EM, de Hoop B, Viergever MA, Prokop M, van Ginneken B. Automatic lung segmentation from thoracic computed tomography scans using a hybrid approach with error detection. *Med Phys* 2009;36:2934–2947.

Electronic Nose Identifies Bronchoalveolar Lavage Fluid Eosinophils in Asthma

To the Editor:

Asthma can be categorized into different inflammatory endotypes based on eosinophilic and/or neutrophilic airway inflammation (1). The type of airway inflammation can predict treatment response to inhaled corticosteroids and biological treatments (1, 2). The gold standard for assessing inflammation in the lower respiratory tract is bronchoscopy and bronchoalveolar lavage (BAL) (3), but this method is invasive and not always well tolerated. Sputum induction and processing is a less invasive alternative, but it is time consuming and the results are not readily available.

Recently, others and ourselves have shown that sputum cell counts are related to exhaled molecular profiles, as measured by gas chromatography–mass spectrometry and by electronic noses (eNoses) (4, 5).

Supported by The Netherlands Lung Foundation grant 3-2-07-012.

Author Contributions: conception and design—N.F., K.F.v.d.S., R.L., J.S.v.d.Z., and P.J.S.; analysis and interpretation—N.F., P.J.S., and A.H.Z.; drafting the manuscript for important intellectual content—N.F., K.F.v.d.S., R.L., and P.J.S.; measurements—N.F., K.F.v.d.S., M.A.v.d.P., A.D., B.S.S., M.B., D.Y., A.W., M.A., H.R., P.B., P.K., L.V., C.M., R.v.S., R.J., and J.S.v.d.Z.

This letter has an online supplement, which is accessible from this issue's table of contents at www.atsjournals.org